

Pressure-induced structural transition and band gap evolution of double perovskite $\text{Cs}_2\text{AgBiBr}_6$ nanocrystals

Ruijing Fu^a, Yaping Chen^a, Xue Yong^b, Zhiwei Ma^a, Lingrui Wang^c, Pengfei Lv^a, Siyu, Lu^b Guanjun Xiao^{a,*} and Bo Zou^a

^a State Key Laboratory of Superhard Materials, College of Physics, Jilin University, Changchun 130012, China

^b College of Chemistry and Molecular Engineering, Zhengzhou University, 100 Kexue Road, Zhengzhou 450001, China

^c Key Laboratory of Materials Physics of Ministry of Education, School of Physics and Engineering, Zhengzhou University, Zhengzhou 450001, China

Corresponding Author

*To whom correspondence should be addressed. Email: xguanjun@jlu.edu.cn

EXPERIMENTAL SECTION

Materials. Cesium acetate (Cs(OAc), 99.9%), silver acetate (Ag(OAc), 99.0%), bismuth (III) acetate (Bi(OAc)₃, 99.9%), trimethylsilyl bromine (TMSB), octadecene (ODE, 90%), oleic acid (OA, 90%), oleylamine (OAm, 80%) were used as received from Sigma and Aldric without further purification.

Synthesis and Characterization of Cs₂AgBiBr₆ NCs. The targeted Cs₂AgBiBr₆ NCs were synthesized according to the modulated colloidal chemistry method. In a typical synthesis, Cs(OAc) (0.1363mg, 0.71 mmol), Ag(OAc) (0.0835mg, 0.5 mmol), and Bi(OAc)₃ (0.1931mg, 0.5 mmol) were dissolved in a combination of 10 mL of ODE, 3 mL of OA, and 1 mL of OAm were loaded in a 25 mL three-neck flask. After degassing for 40 min, the reaction mixture was heated to 110 °C under vacuum for 45 min. The solution thus obtained was heated to 140 °C under a nitrogen atmosphere and neat TMSBr (0.42 mL, 7 mmol) was swiftly injected. After 10 s, the reaction mixture was cooled to room temperature in an ice–water bath. Centrifugation of the reaction mixture and extraction of the resulting precipitate with a small amount of toluene reproducibly allowed the isolation of cube-shaped Cs₂AgBiBr₆ nanocrystals (**Fig. 1**). The resulting samples were characterized by transmission electron microscopy (TEM), high resolution TEM, high-angle annular dark-field scanning transmission electron microscopy (HAADF-STEM) images, and elemental mapping performed on a JEM-2200FS with an emission gun operating at 200 kV.

***In Situ* High-Pressure Optical Experiments.** All of the *in situ* high-pressure experiments shown in this study were carried out with a symmetric diamond anvil cell (DAC) apparatus. Therein, silicon oil with a viscosity of 10 cSt was utilized as the pressure transmitting medium (PTM), which was purchased from Dow Corporation (South Saginaw Road, Midland, MI, USA). The *in situ* high-pressure absorption spectra of Cs₂AgBiBr₆ NCs were recorded with an optical fiber spectrometer (Ocean Optics, QE6500) using a deuterium-halogen light source. High-pressure Raman spectra were recorded using a spectrometer equipped with liquid nitrogen cooled CCD (iHR 550, Symphony II, Horiba Jobin Yvon). The 785 nm diode laser was utilized to excite the

sample and the output power was 50 mw. In situ high-pressure angle-dispersive X-ray diffraction (ADXRD) patterns were obtained with a wavelength of 0.6199 Å at beamline 15U1, Shanghai Synchrotron Radiation Facility (SSRF), China. A focused beam size of about $4 \times 3.5 \mu\text{m}^2$ was adopted for data collection. CeO₂ was used as a standard sample for the calibration of geometric parameters. The Bragg diffraction rings were collected using a Mar-165 CCD detector with an average acquisition time of 10 s for each pressure and then were integrated on the basis of the FIT2D program, yielding 1D intensity versus diffraction angle 2-theta patterns. All the high-pressure experiments were conducted at room temperature.

Computation. The CASTEP module in Materials Studio was carried out for the simulation of the band structure and the partial density of states (PDOS). First-principles density functional theory computations were performed using the plane-wave pseudopotential technique with the generalized gradient approximation (GGA). A plane-wave basis set with an energy cutoff of 765 eV was applied. The PDOS of isolated atoms was collected by adopting the identical pseudopotential of the GGA. Likewise, we re-built nanocrystal model to reproduce the band gap evolution of Cs₂AgBiBr₆ NCs under high pressure. The large unit cell (LUC) method, which is a supercell method is used to model nanocrystals.¹⁻³ The $k=0$ approximation was adopted in the computation. The calculations were performed with the Vienna Ab initio Simulation Package (VASP) which employ plane-wave basis sets, and use the projector augmented wave scheme.⁴⁻⁷ The PBE functional was used. For valence electrons, 5s, 5p, 6s states, and 5d, 6s, 6p states, 4d, 5s states, and 4s, 4p states were explicitly taken into account for Cs, Bi, Ag, and Br, respectively. The Brillouin zone was sampled at a Γ point with a plane-wave expansion cutoff of 550 eV. Such consistency between the calculation of modeling nanocrystal and that of primitive cells just prove our analysis that the band gap broadening of tetragonal phase is due to the distortion of octahedra.

REFERENCE

1. H. M. Abduljalil, M. A. Abdulsattar, and S. R. Al-Mansoury, "SiGe nanocrystals core and surface electronic structure from ab initio large unit cell calculations," *Micro*

and Nano Letters, **2011**, *6*, 386-389.

2. N. A. Nama, M. A. Abdulsattar, and A. M. Abdul-Lettif, "Surface and core electronic structure of oxidized silicon nanocrystals," *Journal of Nanomaterials*, doi:10.1155/2010/952172.
3. M. A. Abdulsattar, "Ab initio large unit cell calculations of the electronic structure of diamond nanocrystals," *Solid State Sciences*, **2011**, *13*, 843-849.
4. G. Kresse and J. Hafner, "Ab initio molecular-dynamics simulation of the liquid-metal–amorphous-semiconductor transition in germanium," *Phys. Rev. B* **1994**, *49*, 14251.
5. G. Kresse and J. Furthmuller, "Efficiency of ab-initio total energy calculations for metals and semiconductors using a plane-wave basis set," *Comput. Mater. Sci.* **1996**, *6*, 15-50.
6. G. Kresse and J. Furthmuller, "Efficient iterative schemes for ab initio total-energy calculations using a plane-wave basis set," *Phys. Rev. B* **1996**, *54*, 11169.
7. P. E. Blochl, "Projector augmented-wave method," *Phys. Rev. B* **1994**, *50*, 17953.

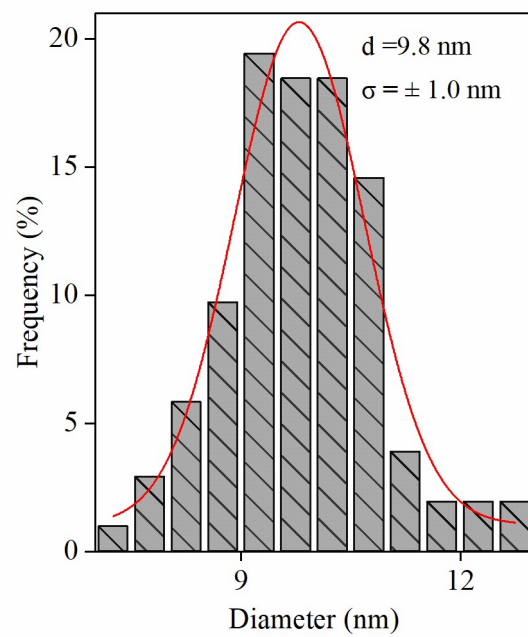


Fig. S1. The corresponding size distribution of as-prepared Cs₂AgBiBr₆ NCs with Gauss fitting.

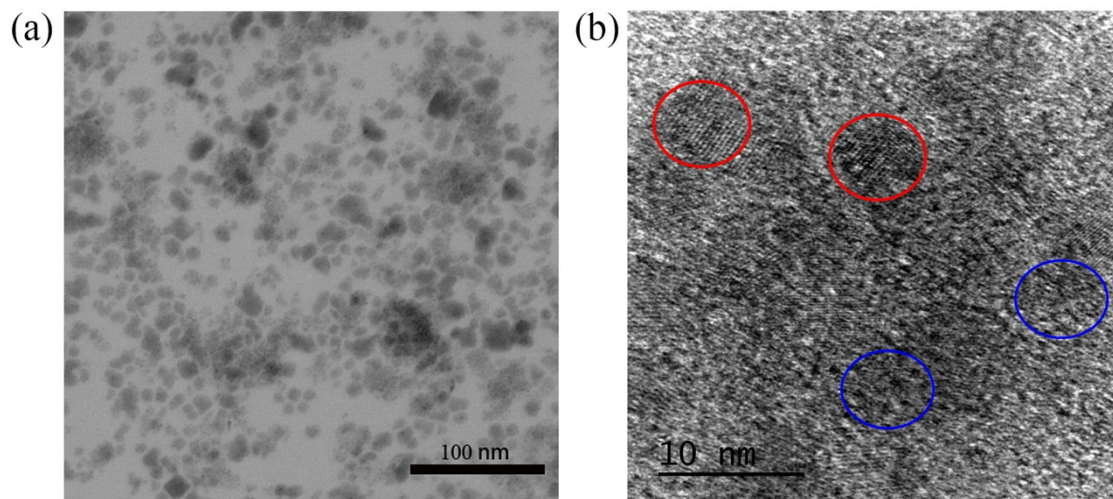


Fig. S2. (a) TEM image and (b) high-resolution TEM image of the $\text{Cs}_2\text{AgBiBr}_6$ NCs when the pressure was completely released to ambient conditions. The red circles represented the amorphous domains, and the blue circles denoted the crystalline domains.

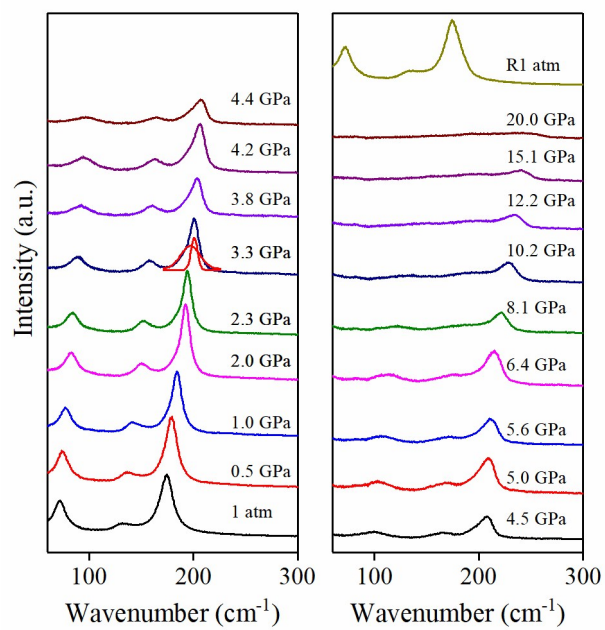


Fig. S3. Selected Raman spectra of Cs₂AgBiBr₆ NCs at elevated pressure.

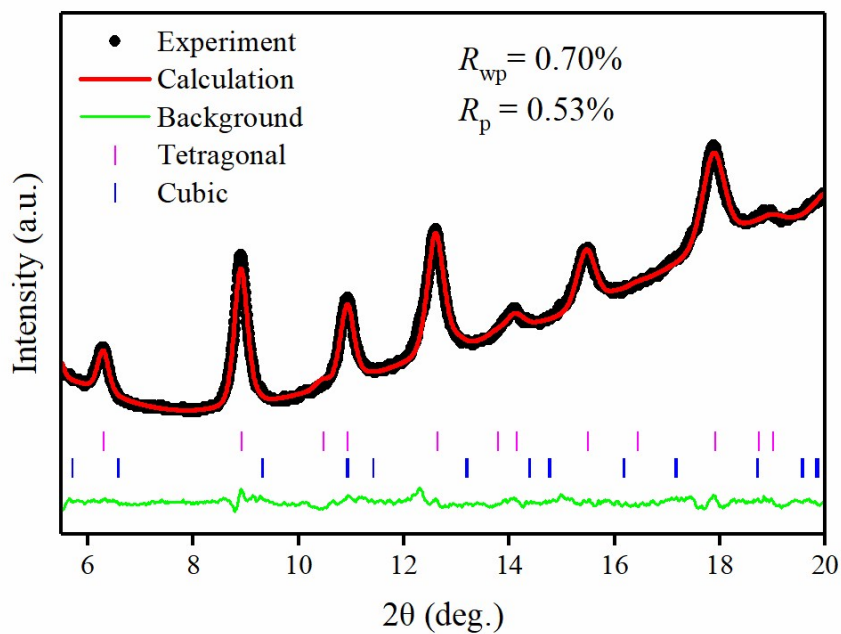


Fig. S4. Refinements of the experimental (black dot), simulated (red line), and difference (green line) ADXR D patterns after decompression to ambient conditions. The blue and pink vertical markers indicate the cubic and tetragonal phase.

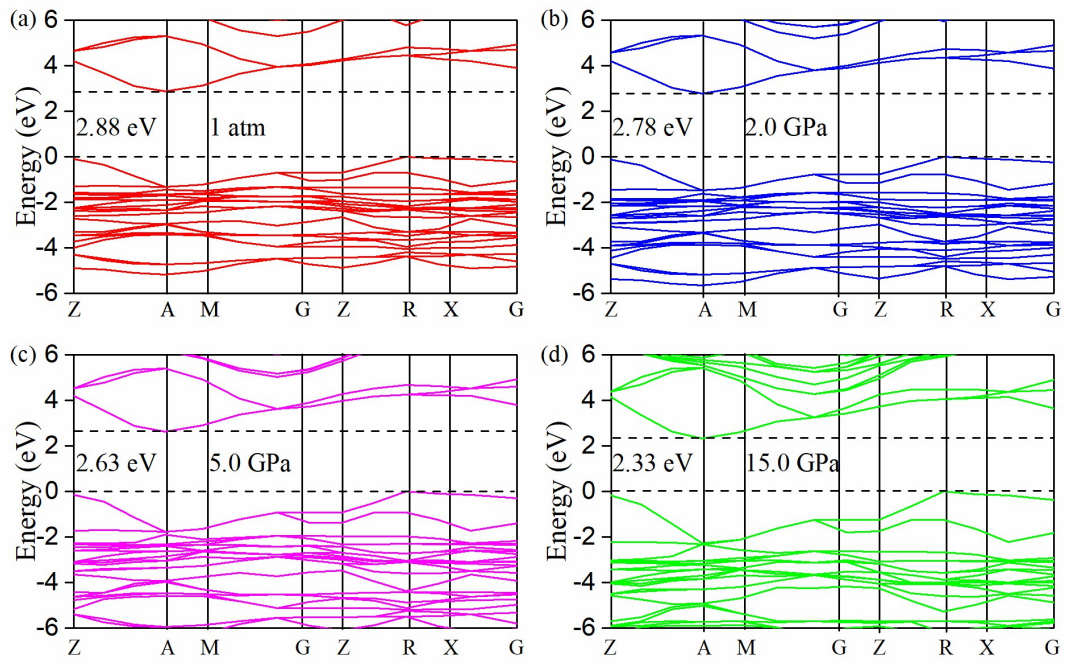


Fig. S5. Calculated electronic band structures of cubic $\text{Cs}_2\text{AgBiBr}_6$ NCs at 1 atm (a), 2.0 GPa (b), 6.0 GPa (c) and 15.0 GPa (d).

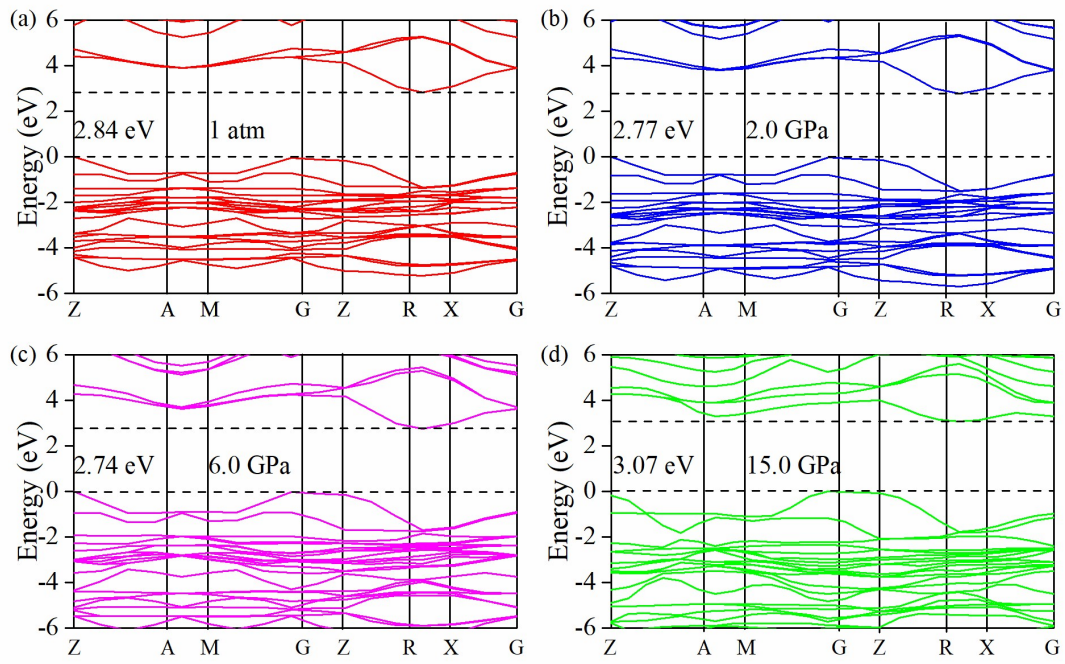


Fig. S6. Calculated electronic band structures of tetragonal $\text{Cs}_2\text{AgBiBr}_6$ NCs at 1 atm (a), 2.0 GPa (b), 6.0 GPa (c) and 15.0 GPa (d).

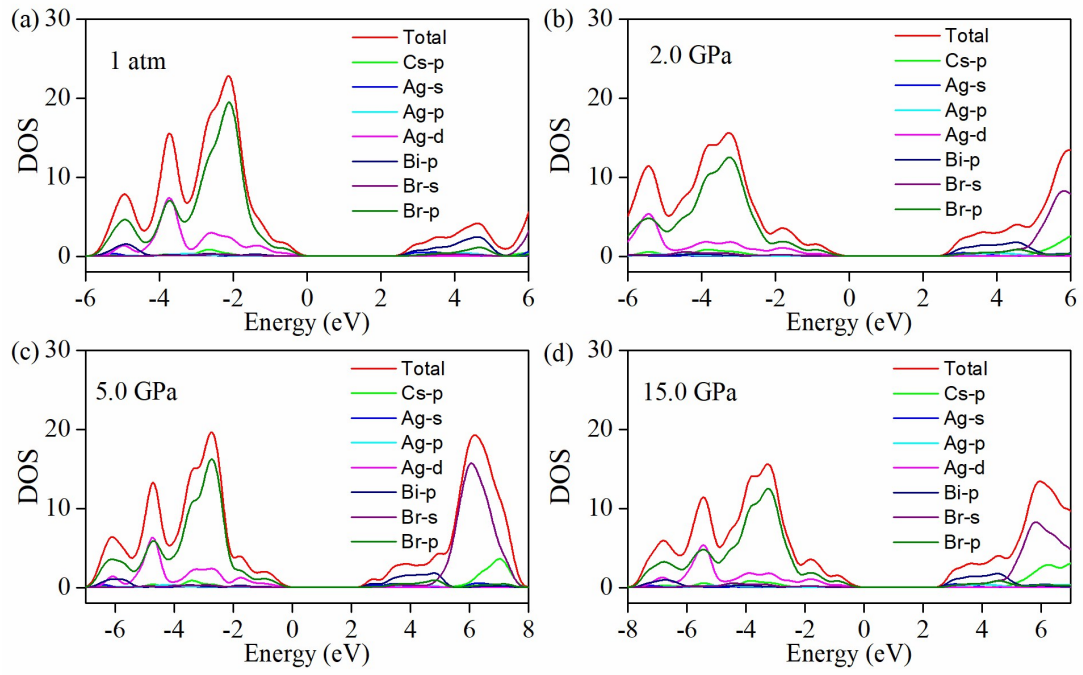


Fig. S7. Calculated partial density of states (PDOS) of cubic $\text{Cs}_2\text{AgBiBr}_6$ NCs at 1 atm (a), 2.0 GPa (b), 6.0 GPa (c) and 15.0 GPa (d).

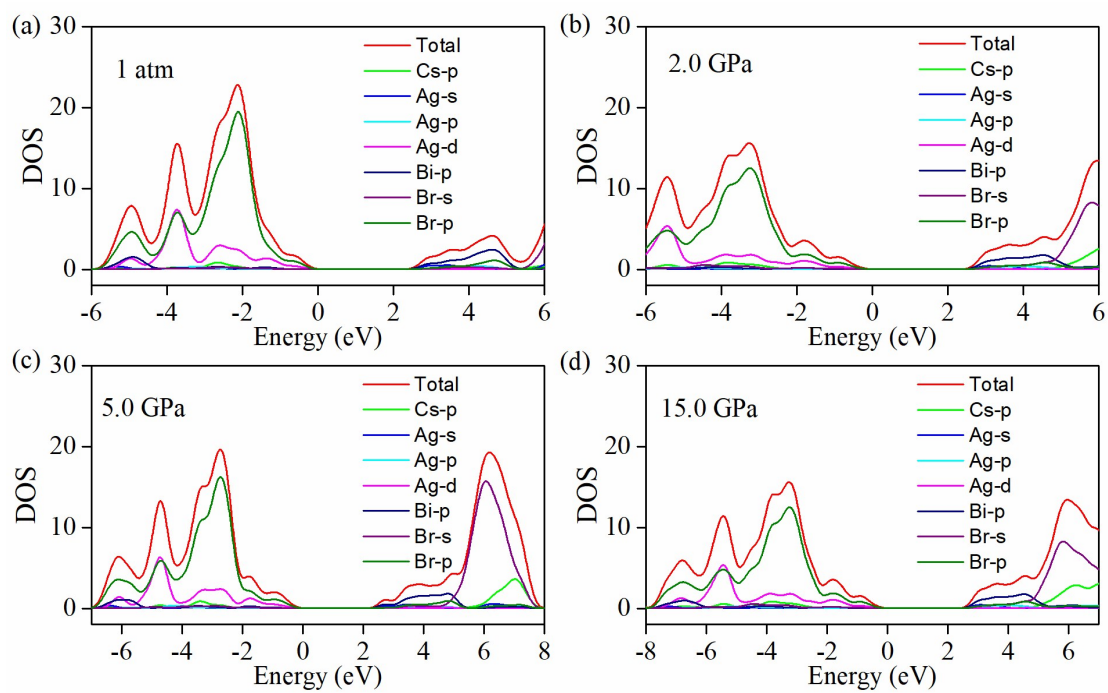


Fig. S8. Calculated partial density of states (PDOS) of tetragonal $\text{Cs}_2\text{AgBiBr}_6$ NCs at 1 atm (a), 2.0 GPa (b), 6.0 GPa (c) and 15.0 GPa (d).

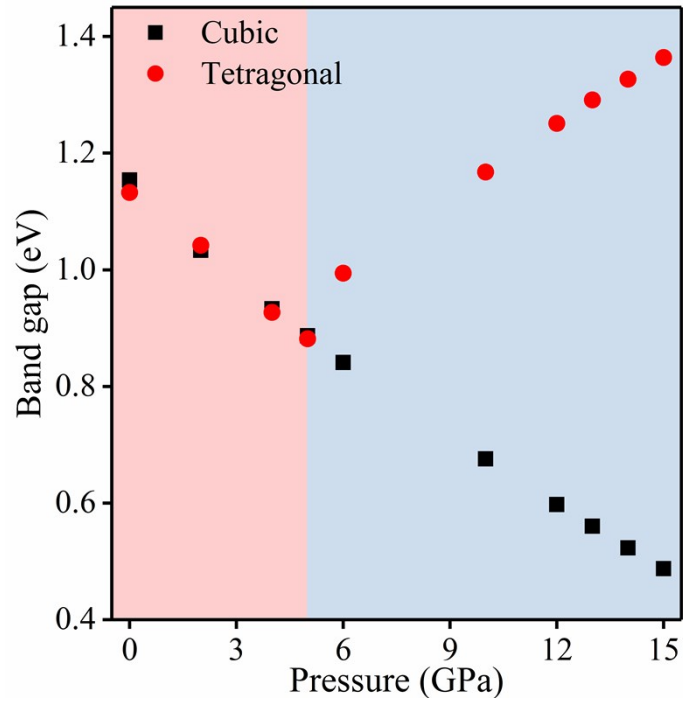


Fig. S9. (a) Calculated band gap evolution of $\text{Cs}_2\text{AgBiBr}_6$ NCs cubic (black) and tetragonal (red) phase at high pressure by using nanocrystal model.